

## WAVE CELERITY FROM VIDEO IMAGING: A NEW METHOD

Rafael Almar<sup>1</sup>, Philippe Bonneton<sup>1</sup>, Nadia Senechal<sup>1</sup> and Dano  
Roelvink<sup>2</sup>

Video systems are emerging tools to monitor high frequency nearshore morphodynamics. Bathymetry can be inverted from surface wave celerity. We present here a new and robust method to estimate this celerity. The method is a time and space cross-correlation based on time-stack images. The celerity estimation is local, within a distance smaller than typical encountered wavelength and uses a time-domain correlation that integrates all wave effects within the duration of the time-stack. A validation is given from available in-situ data of the Pre-ECORS experiment. Global RMS error is lower than 0.2 m/s for the available period of comparison. Thus, the method seems to be well adapted to complex morphologies. Sources of error on the celerity estimation in the nearshore area are also investigated.

### INTRODUCTION

Video imaging has become a predominant monitoring tool for nearshore hydro- and morphodynamics processes (Holland et al., 1997). Bathymetry estimation from video imaging is one of the current nearshore video community challenges. Existing video methods that estimate bathymetry from sea surface are based on wave characteristics evaluation: essentially energy dissipation (Aarninkhof et al., 2003) and wave phase speed (Stockdon and Holman, 2000). Wave energy dissipation method is limited to breaking areas. Thus, for complex nearshore morphologies such as barred beaches, the non-continuous wave breaking reduces the applicability of this method (Aarninkhof et al. 2003). Considering these complex morphologies, wave speed methods can potentially be applied within the whole nearshore area.

Various video imaging methods have been explored to estimate wave celerity or wave number. The subject of our paper is the group of methods based on one-dimensional array of pixel or "time-stack" images. In these images, waves' signature is the temporal variation of pixel intensity associated with the propagation of waves front. Non-breaking waves are identified from the intensity contrast between dark wave front and bright back face. Breaking waves are identified from the intensity peak associated with the bright roller crest due to foam (Lippmann and Holman, 1991). Wave phase signal is then obtained from the pixel intensity signal using a transfer function. The phase of this function is

---

<sup>1</sup> EPOC UMR CNRS 5805, University of Bordeaux, avenue des Facultées, 33405 Talence, France

<sup>2</sup> UNESCO-IHE Institute for Water Education, P.O. Box 3015 2601 DA Delft, The Netherlands

constant in homogeneous zones such as shoaling zone or inner surf zone but locally varies in transitions zones (at the breaking point or when waves stop breaking in troughs). The phase variation is explained by the intensity maximum that shifts from back face of the wave to the roller front (Yoo, 2007).

Three ways to get wave characteristics (celerity ( $c$ ), wavenumber ( $\lambda$ )) from video time-stacks are used in bathymetric inversion studies.

The first type of method is based on a Complex Empirical Orthogonal Function (CEOF) analysis of intensity signal (Stockdon and Holman, 2000). The CEOF technique estimates a wavenumber and a frequency using both space and time domains. The technique works as wave signal is spatially coherent. Thus, technique may have difficulties for barred beaches, where wave signal can change significantly while wave breaks over the bar.

The second type of method is based on individual wave front tracking. In Catalan et al. (2008) breaking wave's fronts are detected as local pixel intensity maxima. Yoo (2007) developed a technique that works both for breaking and non-breaking waves. To remove foam from previous wave breaking and background intensity in shoaling area, intensity peaks are detected in small moving windows. The robustness of these individual wave front tracking methods is uncertain for barred beaches since wave breaking over the bar can lead to harmonics generation but also merging which makes the individual wave tracking inappropriate.

The third type of method is based on intensity timeseries cross-correlation. Time of propagation  $\Delta t$  between two positions  $\Delta x = x_2 - x_1$  is estimated as the maximum of correlation coefficient. Subsequently, celerity is defined as  $C = \Delta x / \Delta t$  (Lippmann and Holman, 1991; Bos, 2006). Spectral-domain cross-correlation has also been applied to video time-stacks to get a local estimation of  $\lambda$  (Plant et al., 2008). These techniques have shown some success in retrieving celerity for barred beaches (Plant et al., 2008). However the assumption of a sinusoidal wave signal associated to spectral method can be discussed while considering the irregular intensity wave signal.

Bathymetry is retrieved from the estimation of wave celerity (or wavenumber) using wave dispersion. On the whole, error on bathymetry estimation from video imaging including celerity estimation and depth inversion ranges between 0.1 m to up to 1 m (Yoo 2007). Error on depth inversion ranges itself between 0.1 and 0.8 m, depending on the complexity of the inversion (linear, non-linear) (Grilli, 1998). Yoo (2007) and Catalan et al. (2008) point out that error coming from the video celerity estimation can be also important. Though, this error remains mainly unknown.

Our motivation is to estimate celerity at barred beaches. Regarding the different assumptions made in existing methods and applicability, we choose to develop a technique based on time cross-correlation, constituting an extension of the method described in Bos et al. (2006). In this paper, field site and video data

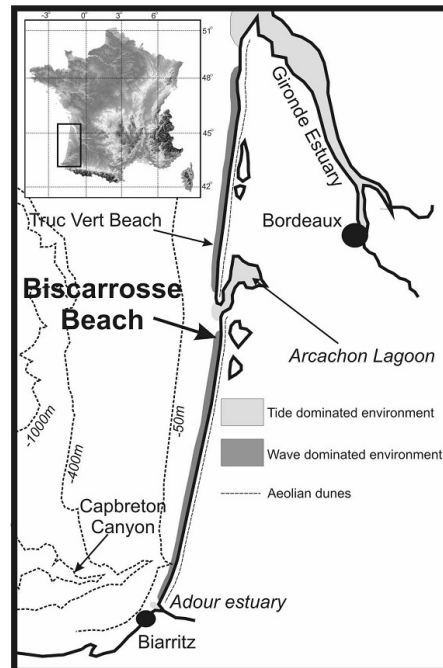


**Figure 1: Localisation of Biscarrosse beach in the South-West of France, facing the North-Atlantic Ocean. The beach is located 30 Km southward of Arcachon Lagoon entrance and is a wave dominated environment.**

are first described. Secondly, our method is described. Finally, a discussion holds on sources of error on celerity estimation from video imaging.

### FIELD EXPERIMENT

The field location used in this study is Biscarrosse Beach located on the sandy Aquitanian Coast, 30 km to the south of the Arcachon Lagoon entrance, France (Figure 1). Biscarrosse Beach is a wave dominated environment which mainly presents a doubled bar system. Over a five-day period in June 2007, morpho- and hydrodynamical data were acquired as part of the Pre-ECORS (SHOM-DGA) experiment (Bruneau et al., 2008). During the experiment, offshore significant wave height ( $H_s$ ) varied from 0.5 m to up to 2.5 m and again less than 1 m within one week (Figure 2). Wave period ranged between 8 s to 11 s and the peak direction was almost shore normal ( $0^\circ - 10^\circ$ ). Tidal range was about 3.5 m.

Synchronised pressure sensor lines were set in the cross-shore direction. Lines locations were chosen for the validation of video celerity estimation at some positions representative of barred beaches. The sampling frequency was set to 8 Hz. The present study is based on a single transect located in a relative alongshore uniform part of the beach. Topography along this cross-shore transect

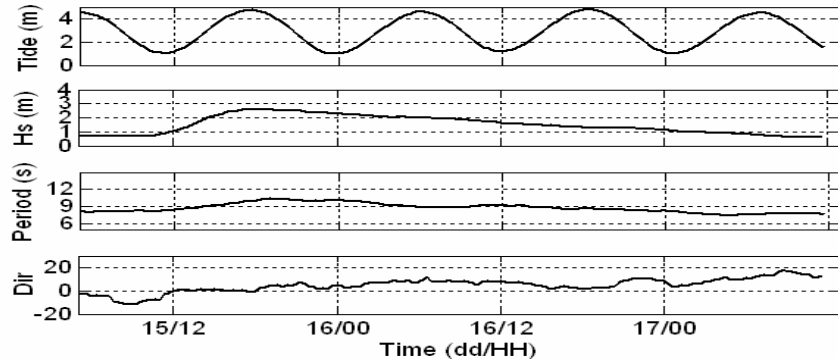


**Figure 2:** Time series of wave and tide conditions during the field experiment Pre-ECORS (SHOM-DGA) at Biscarrosse beach when both video and in-situ data were available. Upper panel is the tidal amplitude, second panel is offshore significant wave height (at 15 m deep), wave period and wave direction from the shore normal direction.

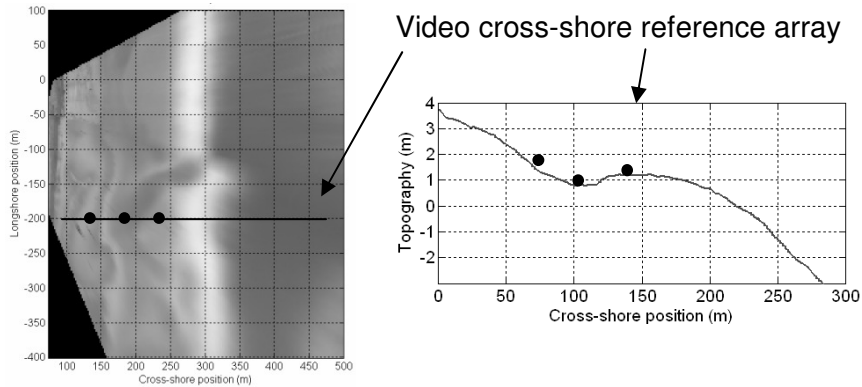


**Figure 3:** Morphology of inter-tidal beach at Biscarrosse during the Pre-ECORS experiment. Left image is a plan view image. Black circles stand for location of pressure sensors and black thick line represents the position of the reference cross-shore array used in our study. Right figure shows the topography along this cross-shore section with the location of sensors in black circles.

is shown on Figure 3. Pressure sensors were positioned as follows: one on the inner shoal, one in the trough and the third one on the upper part of the inter-tidal shoal.

Cross-shore wave celerity was obtained from pressure sensor lines. Celerity was computed with a cross-correlation in time-domain between two different sensors timeseries as explained in Lippmann and Holman (1991). Distance between sensors was around 40 - 50 m which is equivalent or greater than one wavelength

in this area. A pass-band filtering between 0.05 and 0.5 Hz has been applied to data to isolate swell-waves and thus to compute wave celerity.

### VIDEO SYSTEM

A permanent video system CamEra (Coco et al. 2005) has been deployed at Biscarrosse beach in April 2007 (figure 4). Five cameras were positioned at the top of a 12 m pole, located on the eolian dune. The total height above mean sea level is 27 m. Sampling frequency is 2 Hz and three types of images are generated, snapshot images, time-exposure images and 10 minutes time-stacks images. Time-stacks have been positioned to fit the cross-shore pressure lines (Figure 6). In order to describe changes on water level due to the rapid tidal modulation, 4 images per hour are saved. The cross-shore spatial resolution in the inter-tidal area is about 10 cm / pixel.

### METHOD

Existing remote sensing methods that estimate wave celerity are based on the commonly used assumption that video pixel intensity signal can be linked to water level wave signal (Lippmann and Holman, 1991). This assumption has been tested by comparing synchronized timeseries of co-located video pixel intensity and water level from gauge. The Figure 5 shows an example with non-breaking waves. Steep front faces of waves appear as minima whereas mildly sloping back faces are identified as maxima. Basically, intensity and water level signals show similar temporal characteristics but are different in terms of amplitude.

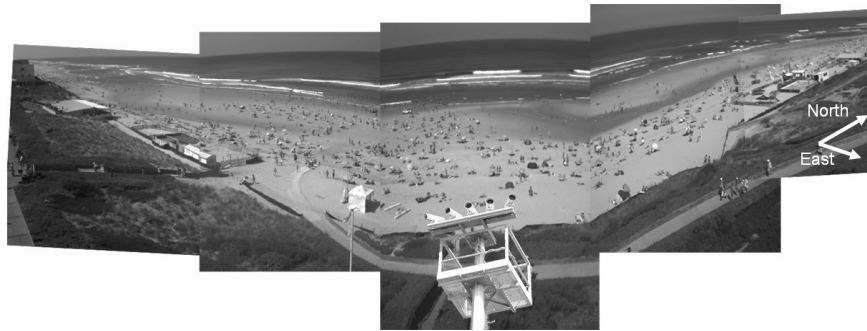
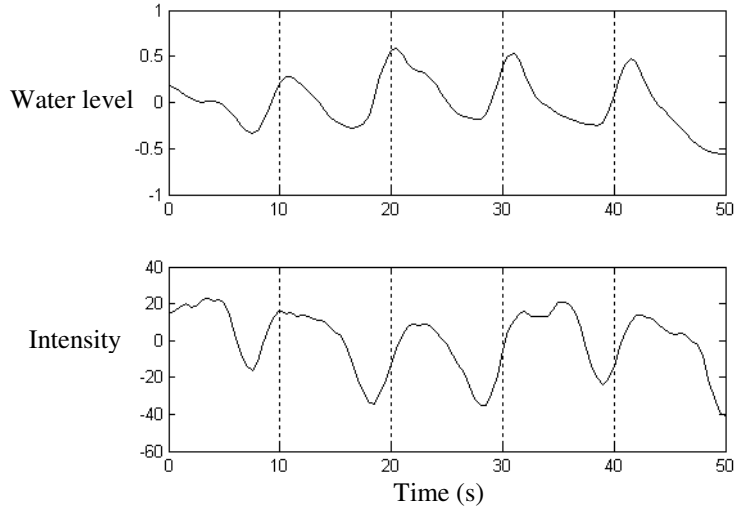
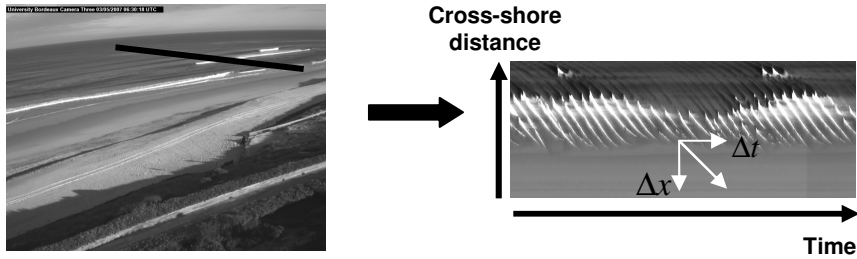


Figure 4: View from the Biscarrosse beach video system. The fifth images are merged. In the lower part is shown the cameras situated at the top of a 12 m pole on the dune.



**Figure 5:** Left hand image shows the location of a pressure sensor line (in white circles). Right hand figure represents synchronized timeseries of water level from a pressure sensor and intensity from video.



**Figure 6:** Left panel is a snapshot image from Biscarosse video system. The cross-shore transect used in the present study appears as a black line. The right panel is a time and space image (timestack) which represents the previous cross-shore section (cross-shore position in the y axis) sampled at 2 Hz during 10 min (time in the x axis).

Images are pre-treated to clean up waves intensity signal. First, a pass-band filter between 0.05 and 0.5 Hz is used to remove low frequency (changing in light due to clouds) and high frequency components (wind-waves or a rapid adjustment of the camera “auto-iris”). Secondly, we have previously seen that intensity amplitude cannot be related to water level amplitude. Hence, to give all waves the same weight, the signal is normalized. The intensity wave signal is then divided by the local intensity maximum.

The method uses both a time and space domains correlation. First, an arbitrary time lag  $\Delta t$  is fixed. For each position  $i$ , a time-domain cross-

correlation is computed with neighbour positions  $\mathbf{j}$  from  $\mathbf{1}$  to  $\mathbf{n}$ , using the previously fixed  $\Delta t$ :

$$\text{Cor}_i(\mathbf{j}) = \langle X_i(t) \cdot X_{\mathbf{j}:n}(t+\Delta t) \rangle$$

The resulting  $\text{Cor}_i(\mathbf{j})$  is obtained for each of the neighbour positions  $\mathbf{j}_{1:n}$  (Figure 7). The index of the maximum of correlation gives an estimate of the time-integrated distance made by waves during  $\Delta t$ . These steps are repeated for each of the positions  $\mathbf{i}$ .

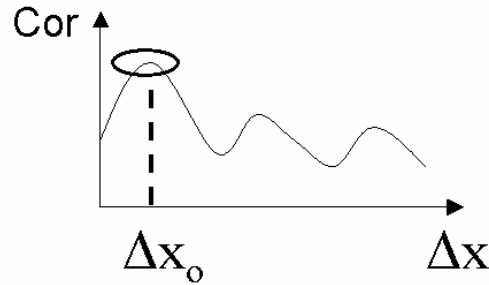


**Figure 7: Representation of the correlation coefficient between a given position and neighbor positions as a function of the distance  $\Delta x$ . The value  $\Delta x_0$  is the index of the position that is associated with the maximum of correlation.**

Thus, we get a local estimate of the celerity as  $C = \Delta x_0 / \Delta t$  (Figure 6).

It is commonly admitted that wave shape does not change significantly over a distance lower than one wavelength  $O(10 - 40 \text{ m})$ . Also, minimum wavelengths are associated with shallower water levels. Thus, if we fix  $\Delta t = 1 \text{ s}$ , the distance made by the wave during  $\Delta t$  is  $\sim 2 \text{ m}$  which is much smaller than the wavelength ( $\lambda \sim 10 \text{ m}$  for  $T \sim 5 \text{ s}$ ). Hence, we consider that wave's shape change is not an issue in our method.

Finally, the method can be applied to both cross-shore and alongshore celerities to compute a propagation angle.

### Validation

The method has been validated using Pre-ECORS data. The figure 8 shows two test cases of timestack images located on the reference cross-shore transect (figure 3).

Figure 8.a represents a test case for swell-waves ( $H_s \sim 1 \text{ m}$ ) and high tide conditions. Left panel is the original timestack image. Central panel represents the correlation coefficient computed for each position (horizontal dimension) and distance  $\Delta x$  from this position (vertical dimension). The coefficient maximum clearly appears at all the positions. Right panel shows the original image in which the wave celerity has been removed. If wave celerity is well estimated, wave trajectories should appear horizontally. The horizontal wave's trajectories indicate that wave celerity is well estimated at all the positions.

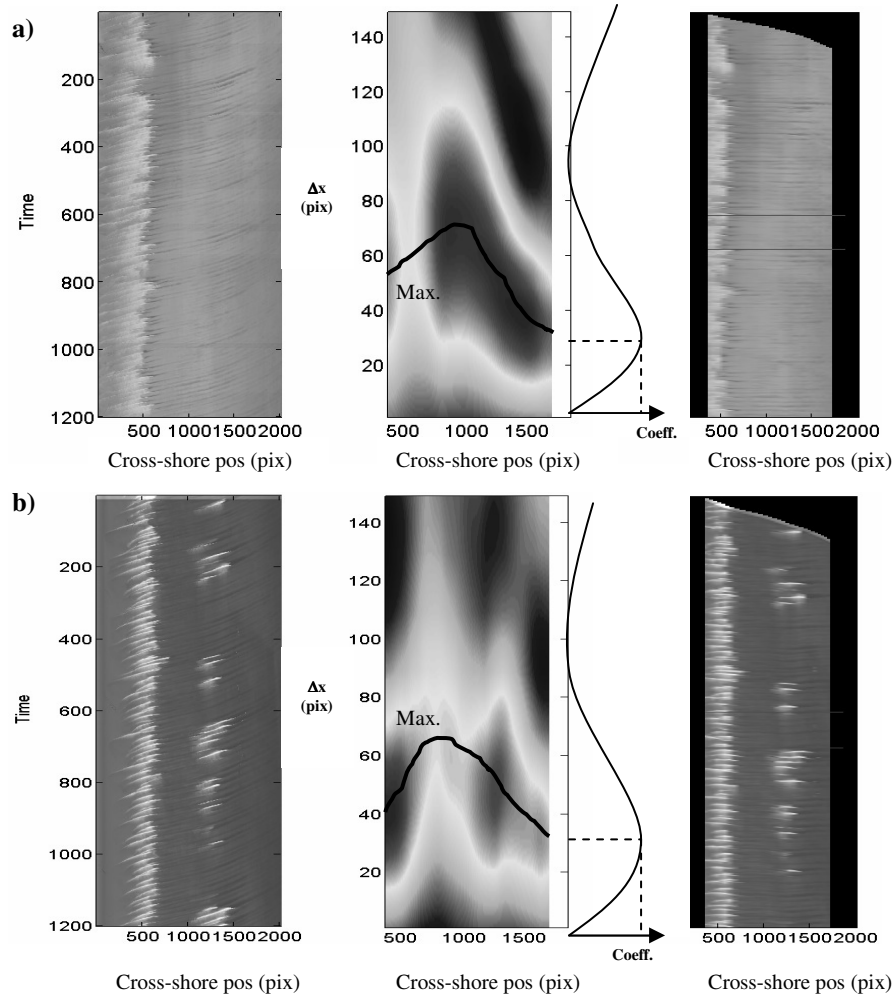


**Figure 8:** a) image is taken for high tide while waves do not break over the inner bar whereas lower figure b) is taken at mid tide when intermittent breaking occurs. Left panel image is a time-stack along a cross-shore array. Central panel represents the correlation coefficient computed using our method for each cross-shore position (horizontal - in pixel) and each distance from this position (vertical - in pixel). Black line on the right side represents an example of the correlation coefficient at a position as a function of the distance from this position. Right panel shows the initial time-stack in which wave estimated celerity has been removed. If celerity is well estimated, wave trajectories are horizontal. In all of these panels, positions are expressed in pixels, so the reader has to keep in mind that pixel resolution is not constant and varies from about 10 cm to 5 m far away from the camera.

A second test case is shown in Figure 8.b for small swell-waves ( $H_s \sim 1$  m) close to mid-tide with an intermittent wave breaking over the inner-bar. Correlation coefficient in central panel shows a maximum that is not as sharp as in the previous test case. Coefficient pattern presents maxima in homogeneous areas such as surf zone, breaking zone over the bar and in shoaling zones. This coefficient is lower in transition zones like breaking point or in the through where waves stop breaking. In spite of this, the right panel shows that the wave celerity is well estimated at all the positions.

In addition, a comparison between in-situ computed and video estimated celerity is shown on figure 8. The validation is held during three periods of the experiment when both video and in-situ data are available. Wave conditions varied from significant wave height lower than 1 to up to 2.5 m for periods from 8 to 11 s. Spring tide conditions made the water level to vary up to 4 m. Time series of celerity show that our video estimation is close to the in-situ computed celerity for various wave and tide conditions. The mean RMS error on the celerity estimation is lower than 0.2 m/s. Yet, for some reasons, the error can be locally important as encountered the 16<sup>th</sup> of June around mid tide (error greater than 0.4 m/s).

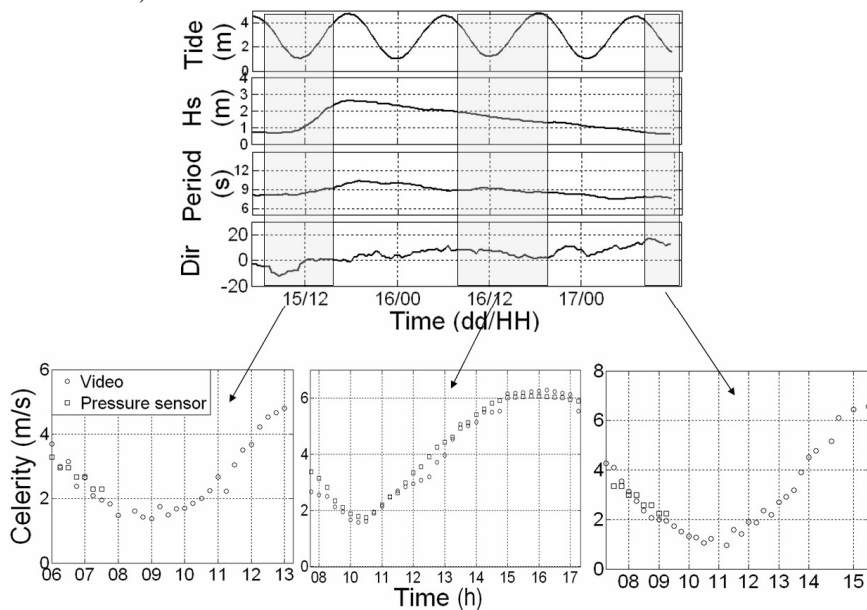


**Figure 9: Upper panel reminds wave and tide forcing during the Pre-ECORS experiment. Yellow periods show periods for which we had both video and in-situ measurement of wave celerity. The three bottom panels show timeseries of wave celerities computed from pressure sensors (squares) and from video using our method (circles)**

## DISCUSSION

Although the global accuracy of video methods for celerity estimation, error can be locally and punctually important. In particular, a complex morphology and shallow water can lead to important errors. These errors come from the increased difference between wave water level signal and video intensity signal. This can be explained by the fact that in video signal, steepest waves have the strongest signal and main incident wave signal can be dominated by steep harmonics waves (Figure 10.a). Furthermore, harmonic generation can be strong after wave breaking over the inner bar or for a sharp variation of topography (Masselink, 1998; Senechal et al, 2002). For instance, spectra shown on Figure 10.b illustrate the difference between in-situ and remote sensing data. While harmonics represent less than 1/5 of main peak waves in the in-situ spectrum, it reaches 1/2 in the video data.

An important error common to video celerity methods can also occurs at transition zones such as the breaking point or when waves stop breaking in the trough. At these positions, the transfer function between wave phase signal and video signal shifts sharply: the maximum of intensity moves from back face of waves for the shoaling zone to the front face for breaking waves. This leads locally to an artificial over- or under-estimation of the video celerity.

In our method we have tackled and fixed some issues specific to video celerity estimation in a complex morphology. Celerity is estimated within a distance lower than a wavelength. This implies that it does not need a global coherence of the wave signal as require EOF based methods. The local estimation of the celerity makes our method appropriate when wave signal is not continuous from offshore to the inner surf zone, for instance at low tide for a complex morphology. In addition, in our method, the time-domain correlation which is preferred to spectral-domain makes the method robust for various intensity wave shapes. This characteristic has to be considered because wave intensity signal in nearshore area is often far from a sinusoid.

Furthermore, all waves within the time-stack duration are integrated to estimate a single celerity. This can be important in case of a weak wave signal or intermittent breaking allowing a robust estimation of the celerity. This also can be an important point in shallow water, especially when individual wave celerity is variable due to amplitude dispersion.

Application of our method to a wider range of wave conditions and other sites would extend the validation. In particular, swell spectrum was very narrow banded during Pre-ECORS with swell-waves. For more complex conditions like an addition of incident swells or wind- and swell-waves as found in North Sea, celerity could be trickier to determine. For instance, computing an average celerity for two swells coming from two different directions is somehow ambiguous. To tackle this issue, our method could be tested computing several celerities related to very narrow frequency bands.

Our final aim in video remotely sensing wave celerity is assimilation in a numerical model or an inversion to estimate topography. In this perspective, an

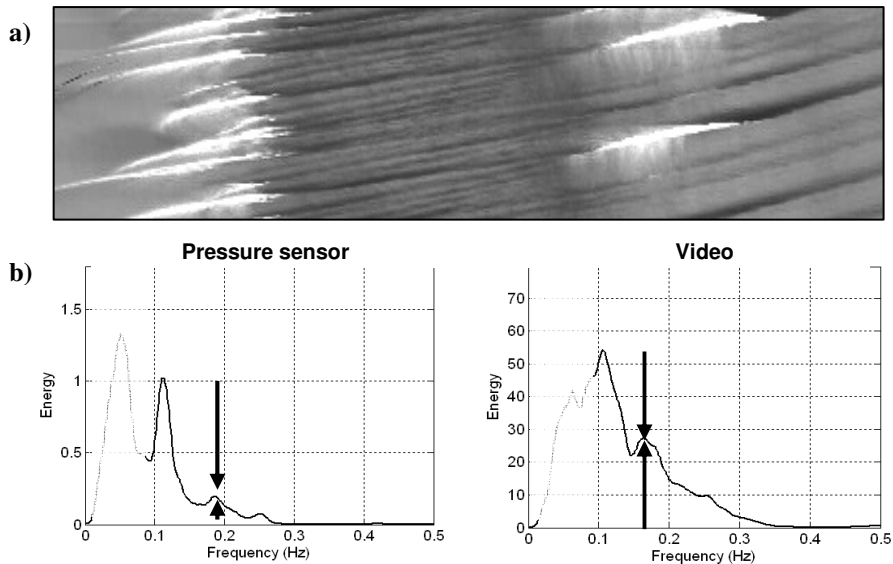


**Figure 10: Sources of errors on the video celerity estimation. a) Upper panel is a time-stack image with time in the y axis and cross-shore position in the x axis. Breaking is intermittent over the inner bar and harmonics are clearly visible in the through. Merging is also visible in the inner surf zone while approaching the swash zone. b) Lower panels are two spectrums computed in the trough at mid-tide, left spectrum is computed from a pressure sensor and right one is from video intensity signal. Arrows show the relative amplitude of harmonics component when compared to the main peak.**

estimation of the uncertainty on the video celerity estimation is required. A way to compute the uncertainty would be to get the width of the maximum peak of correlation coefficient at each location (Figures 7 and 8). For instance the reference proxy can be the width in pixel of the main peak at  $2/3$  of the maximum coefficient value. Then, knowing the pixel resolution (m/pixel) and the fixed  $\Delta t$ , this distance can then be turned into an error in m/s for each location.

## CONCLUSIONS

A new method was developed for the estimation of nearshore wave celerity from video imaging. This method is based on time-stack images and requires a pre-treatment consisting in a pass-band filtering and normalization. The method uses both on time and space correlation and the celerity estimation is local which allows a usage for various shapes of wave signal and barred beaches. In addition, a single celerity is estimated by integrating several waves' effect which makes the method robust for intermittent breaking or weak wave signal. Remotely sensed celerity has been validated using Pre-ECORS in-situ data. During the experiment, wave conditions varied from 1 to up to 2.5 m and tidal range was about 4 m. Over the three days of validation, difference between measured and

estimated celerities remained lower than 0.5 m/s with an average difference lower than 0.2 m/s. However, errors common to all video celerity methods arise from barred beaches specificities, harmonics generation and variation of the transfer function between pixel intensity and water level wave signal. Finally, our simple and robust method should be taken into consideration and tested for estimating high frequency nearshore complex morphology.

#### ACKNOWLEDGMENTS

The Biscarrosse video system was funded by the Aquitaine Region, the Pre-ECORS experiment was supported by the SHOM-DGA and the BRGM. Video system was installed in collaboration with the NIWA (NZ). Almar R. PhD thesis is funded by the Délégation Générale de L'Armement (DGA).

#### REFERENCES

- Aarninkhof, S. (2003): Nearshore Bathymetry derived from Video Imagery. *Delft University of Technology PhD Thesis*
- Bos, C. Wave characteristics derived from video, *Delft University of Technology Master Thesis report*, 2006
- Bruneau, N.; Castelle, B.; Bonneton, P.; Pedreros, R.; Almar, R.; Bonneton, N.; Bretel, P.; Parisot, J. & Senechal, N. : Field observations of intense rip current on a well-developed Transverse Bar and Rip system, *Submitted to Continental Shelf Research*, 2008
- Catalan, P. & Haller, M. Remote sensing of breaking wave phase speeds with application to non-linear depth inversions *Coastal Engineering*, 2008, 55, 93-111
- Coco, G.; Bryan, K.; Green, M.; Ruessink, B.; Turner, I. & van Enckevort, I. Video observations of shoreline and sandbar coupled dynamics *Proceedings of Coasts and Ports 2005, Adelaide*, 2005, 471-476
- Grilli, S. and Skourup, J. Depth inversion for nonlinear waves shoaling over a barred-beach *Proceedings, 26<sup>th</sup> International Conference on Coastal Engr. ASCE*, 1998, 603-616
- Holland K.T., Holman R.A., Lippmann T.C., Stanley J. and Plant N., Practical use of video imagery in nearshore oceanographic field studies, *IEEE Journal of Oceanic Engineering* 22 (1997) (1), pp. 81-92.
- Lippmann, T.C., and Holman, R.A. (1991): Phase speed and angle of breaking waves measured with video techniques; *Proc. Coastal Sediments '91, New York: ASCE*, pp. 542-556.
- Masselink, G. Field investigation of wave propagation over a bar and the consequent generation of secondary waves, *Coastal Engineering*, 33:1, pp 1-9 (1998)
- Plant, N. G.; Holland, K. T. & Haller, M. C. Ocean Wavenumber Estimation From Wave-Resolving Time Series Imagery *IEEE Transactions on Geoscience and Remote Sensing*, 2008, 46, N°9

- Senechal, N.; Bonneton, P. & Dupuis, H. Field experiment on secondary wave generation on a barred beach and the consequent evolution of energy dissipation on the beach face *Coastal Engineering*, 2002, 46, 233-247
- Stockdon H.F., Holman R.A. (2000): Estimation of Wave Phase Speed and Nearshore Bathymetry from Video Imagery, *Journal of Geophysical Research*. Vol. 105, No. C9, pp 22,015-22,033.
- Yoo, J. Nonlinear Bathymetry Inversion Based on Wave Property Estimation from Nearshore Video Imagery *PhD report of the Georgia Institute of Technology*, 2007

KEYWORDS – ICCE 2008

Wave celerity from video imaging: A new method

Rafael Almar, Philippe Bonneton, Nadia Senechal and Dano Roelvink

Abstract 539

Wave celerity

Video imaging

Cross-correlation

Time-stacks

Remote sensing

Nearshore bathymetry